SCIENTIFIC PAPERS
OF THE UNIVERSITY OF PARDUBICE
Series A
Faculty of Chemical Technology
10 (2004)

CHOLESTERIC FINGERS. A REVIEW

Slavomír PIRKL[a1] and Patrick OSWALD[b]
[a]Department of Physics, The University of Pardubice, CZ–532 10 Pardubice,
[b]Ecole Normale Supérieure de Lyon, Laboratoire de Physique,
FR-69364 Lyon Cedex 07

Received September 29, 2004

The behaviour of a cholesteric liquid crystal subjected to a topological frustration together with an a.c. electric field is described. The frustration comes from the homeotropic anchoring of the molecules on the two electrodes limiting the sample. This geometrical boundary condition is incompatible with the helical structure of the phase. As a result, the helix can partly unwind to form "cholesteric fingers" (CF) of different types in coexistence with the homeotropic nematic phase. We review their static and dynamic properties in electric field.

Introduction

Cholesteric liquid crystals were known for a long time to form spectacular patterns. One of them is the fan-shaped texture observed as early as 1922 by G. Friedel [1]. Another variant of this pattern are the "polygonal fields" described by Y. Bouligand [2]. Cholesterics can also form "fingerprint textures" when they are

[1] To whom correspondence should be addressed.

sandwiched between two surfaces treated *via* homeotropic anchoring (molecules normal to the surfaces). In that case, the texture is composed by the so-called "cholesteric fingers" (soliton-like solutions). This texture was first observed by Brehm *et al.* in 1974 [3] close to nematic-cholesteric phase transition. At the same time, "spherulites" (or "cholesteric bubbles") were described by Kawachi *et al.* [4] and by Haas and Adams [5] in similar samples. The structure of the cholesteric fingers was calculated numerically (by assuming isotropic elasticity) by Press and Arrott two years later [6,7], while different (inexact) models were proposed for the spherulites at the beginning of the 1980's [8,13–15].

The problem of cholesteric fingers then fell into oblivion till 1994, when we discovered that another type of fingers as those described by Press and Arrott (called CF-1 hereafter) could exist in the samples [9]. Our main result was that these new fingers (named CF-2) were able to drift perpendicularly to their axes in a.c. electric field and form spirals. In addition, they could break in small pieces in a strong electric field which then form spherulites, in contrast to CF-1's which always collapse at similar conditions. Four years later, we observed that two other kinds of fingers may form in samples, we called them respectively CF-3 and CF-4 [10].

In this article, we review the main properties of these different types of fingers.

Background on the Cholesteric Phase and its Unwinding Transition

The cholesteric phase is a nematic-type liquid crystal composed of optically active molecules. The director $\boldsymbol{n}$ (that locally gives the preferred molecular direction, with $\boldsymbol{n} \Longleftrightarrow -\boldsymbol{n}$) is perpendicular to a helical axis along which it rotates with a spatial periodicity $p/2$ (p is the cholesteric pitch corresponding to a 2π-rotation of the director). Such a structure can also be obtained by adding a small quantity of a chiral substance to a nematic phase. In this case, the helical pitch p depends on the concentration c of the chiral substance (at low c, p is proportional to $1/c$).

The helical structure of cholesteric phase can be unwound by confining the sample between two glass electrodes, treated for the homeotropic anchoring. These boundary conditions are topologically incompatible with the helical structure of the phase and generate a frustration that tends to unwind the phase [10–12]. The nematic phase forms when the confinement ratio between the sample thickness, and the equilibrium pitch ($C = d/p$) is typically close $C_c \approx 1$. This can be seen immediately by performing a wedged sample (Fig. 1): in the thinnest part, the nematic phase forms (black region R1) while fingers invade the sample in the thickest part. Note that the nematic phase is still visible between the fingers in region R2, whereas it completely disappears in region R3.

At large confinement ratio ($C > C_c$), the cholesteric phase can still be un-

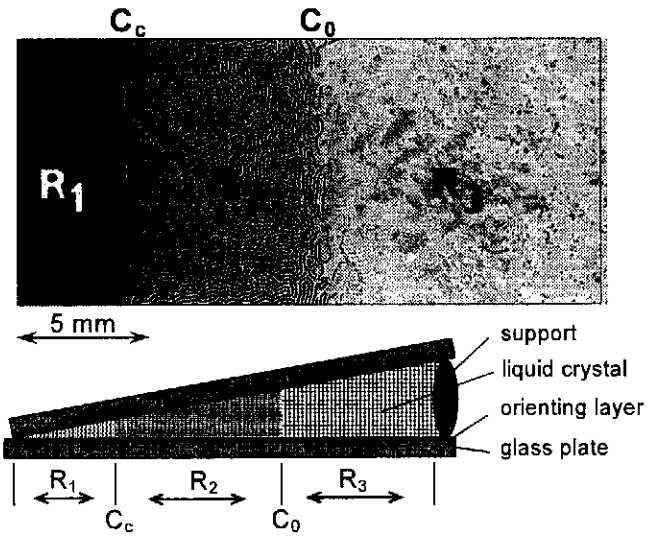

Fig. 1 Cholesteric phase sandwiched between two glass plates treated for homeotropic anchoring and making a very small angle α (From Ref. [12]): a) Three regions are visible from the left to the right between crossed polarizers: R1–homeotropic nematic phase, R2–cholesteric fingers (CF1's) separated by nematic phase, R3–cholesteric fingers without nematic phase in between (the molecules are no longer oriented in homeotopic anchoring along the sides of the fingers); b) Cross-section of the cell

wound by applying an electric field, provided that the liquid crystal is of positive dielectric anisotropy ($\Delta\varepsilon = \varepsilon_{/\!/} - \varepsilon_{\perp} > 0$) [13–15].

Conversely, an electric field allows us to restore the cholesteric phase from the nematic phase if the liquid crystal is of negative dielectric anisotropy [16–18] but we will not discuss this problem here.

The unwinding transition is usually sub-critical (i.e. first-order in the language of phase transitions) due to the elastic anisotropy of the cholesteric phase [19] (this important point was not mentioned in the pioneering papers of the seventies) and is controlled by two parameters: the confinement ratio C and the voltage V applied across the electro-optic cell [16,20]. If the sample is thick enough and the electric field has intermediate values, then usual cholesteric fingers (CF-1) occur, which can grow separately or by forming a dense periodic array. In the phase diagram of Fig. 2, isolated fingers are observable between lines $V_2(C)$ and $V_1(C)$: in this region, the fingers are surrounded by the homeotropic nematic phase and elongate during their growth process (see Fig. 5a). Between $V_1(C)$ and $V_0(C)$, they split and can form a dense periodic pattern (see Fig. 5b, c). In this region, they are still separated by a thin band of homeotropic nematic phase. The optical contrast of the CF1's between crossed polarizers is rather complicated and

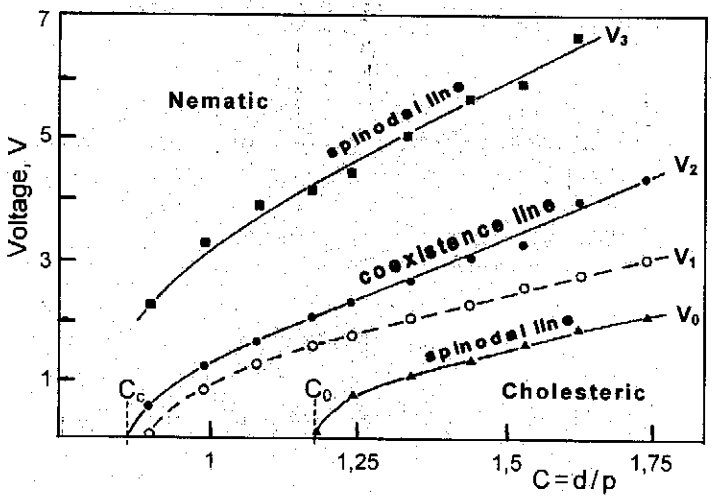

Fig. 2 Typical phase diagram showing that the nematic-cholesteric phase transition is first-order (mixture ZLI2452/ZLI 811) [20]

was analysed in Ref. [21]. Below $V_0(C)$, the nematic phase is no longer visible between the fingers. In this region, the nematic phase is completely unstable: as a consequence, $V_0(C)$ marks the spinodal limit of the nematic phase. A fourth line $V_3(C)$ is reported in the phase diagam: it corresponds to the spinodal limit of the fingers. Note that $V_2(C)$ is the *coexistence line* between the fingers and the nematic phase. That means that on this line, the cholesteric fingers have exactly the same energy as the nematic phase. As a consequence, an isolated cholesteric finger does not change its length at this voltage. Let us emphasize again that this phase diagram is relative to continuous CF1's whose topology was first described by Press and Arrott [6,7].

It turns out that besides CF-1's and cholesteric bubbles discovered in the 1970's, at least 3 other types of fingers can nucleate [10], with very different static and dynamical properties. This point is detailed in the following paragraph.

Other Cholesteric Fingers. Preliminary Observations

Cholesteric fingers of the first and of the second species (CF-1 and CF-2) were distinguished for the first time by analysing their dynamical properties in a low frequency a.c. electric field. The reason why CF-2's were confused with CF-1's during many years is that their optical contrasts are very similar despite very different molecular structures. Using videomicroscopy and image analysis, we

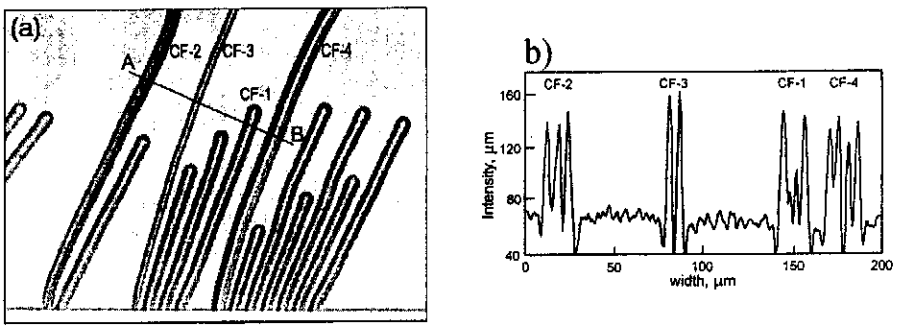

Fig. 3 (a) The four types of isolated fingers that can nucleate from the front with the isotropic liquid. Observation in directional solidification of the cholesteric phase into its isotropic liquid (non polarised light). (From Ref. [10]); (b) Intensity profile across line A - B

found that both types of fingers move very slowly in samples while keeping a constant length in a low-frequency electric field [9]. The crucial point is that CF-1's crawl along their axes, whereas CF-2's drift perpendicularly to their axes. Note, in addition, that below the coexistence voltage (which is slightly lower for the CF-1's than for the CF-2's) the fingers lengthen, whereas above it, they shorten. Finally, these two types of fingers can form closed loops.

More recently, two additional types of isolated fingers (CF-3 and CF-4) were observed, firstly by using directional solidification of the cholesteric phase into its isotropic liquid and secondly in ordinary electro-optic cells [10]. The four types of fingers are clearly identified in Fig. 3. The CF-3's are the thinnest ones while the CF-4's are the thickest ones.

The different fingers can also transform into each other depending on the voltage. For example, we have observed transformation $CF-2 \rightleftarrows CF-3$ (reversible), $CF-4 \rightarrow CF-2$ (irreversible) and $CF-4 \rightarrow CF-3$ (irreversible) [10].

CF-1 Fragments and Loops

The cholesteric fingers of the first type (or CF-1) are the most common. They continuously form from the nematic phase, which shows that their director field is continuous, without any singularities. They never drift perpendicularly to their axes in a.c. electric field. This is a direct consequence of their invariance by a π rotation around their long axes (Fig. 4). A segment of a CF-1 spontaneously collapses above the coexistence voltage V_2 whereas it lengthens from its two ends while undulating below (Fig. 5a). We emphasise that due to the absence of mirror symmetry in a cholesteric phase, the two ends of a CF-1 segment are different (one

is sharp whereas the other is rounded [20,22]). As a result, a segment of a CF-1 can "crawl" along its axis in a.c. electric field, which was really observed experimentally in the conducting regime [9]. Note that voltage V_2 is usually defined as the voltage at which long fragments of CF-1 (i.e. of length much larger

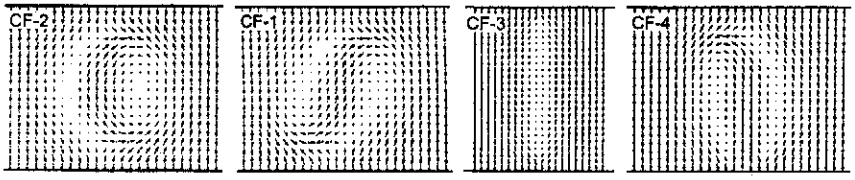

Fig. 4 Director field inside cholesteric fingers CF-1 , CF-2 , CF-3 and CF-4 calculated numerically (cross-section perpendicular to the finger axis). (From Refs [10,25,33])

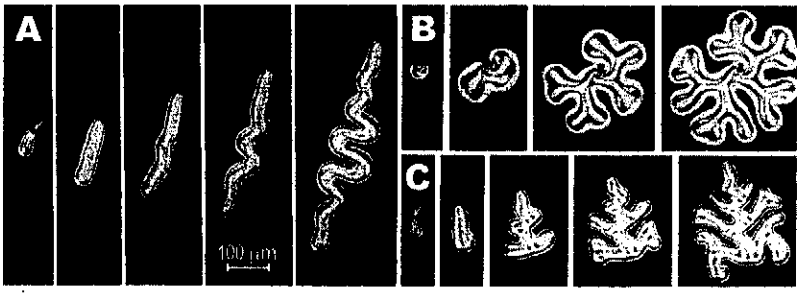

Fig. 5 A) Undulating cholesteric finger of the first type (CF-1); B) CF-1 with two rounded (normal) tips. This finger necessarily contains a point defect (here a dust) which is well visible in the photographs; C) Splitting CF-1 with two different tips. The arrow marks the sharp (abnormal) tip. Crossed polarizers. (From Ref. [24])

than their width) crawl along their axes while keeping a constant length. That means that their two tips move with opposite velocities, i.e. $v_{rounded\ tip} = -v_{sharp\ tip}$ (Fig. 6). This motion is clearly due to an electrohydrodynamic coupling between the electric field, the charges (impurities contained in the liquid crystal) and the director field inside the finger. The crucial role of the electric conductivity is shown in Fig. 13.

The rounded (normal) tip can also split if the voltage is low enough whereas the sharper (abnormal) one always remains unchanged during the growth. Typical behaviour can be seen in Fig. 5b,c.

Recently, it has been observed that very short CF-1 "drop-like" fragments can also exist in a narrow range of voltage above the coexistence voltage ($V_2 < V$

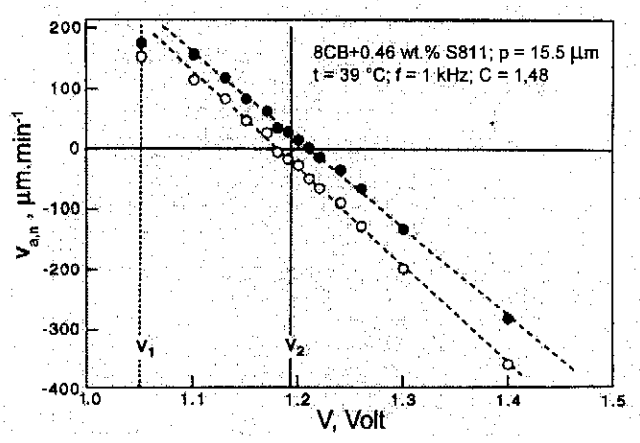

Fig. 6 Velocities of the normal (○) and abnormal (•) tips of the CF-1's as a function of the applied a.c. voltage. (From Ref. [9])

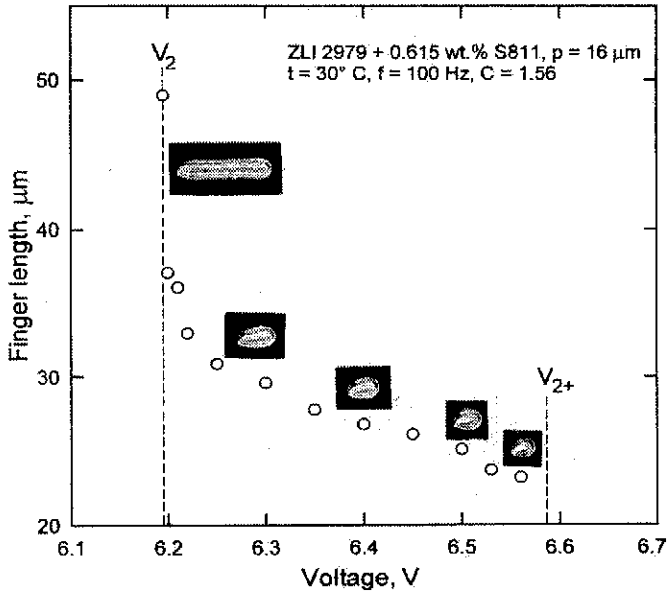

Fig. 7 Length of the CF-1 fragments as a function of the applied a.c. voltage in a two-frequency cholesteric mixture. The frequency is smaller than the charge relaxation frequency.

$< V_{2+}$). Their length depends on the voltage and diverges when $V \to V_2$ [23]. Above voltage $V_{2+}(C,f)$ (where f is the frequency) they collapse (Fig. 7). This solution seems to be specific for the so-called two-frequency mixtures whose ty-

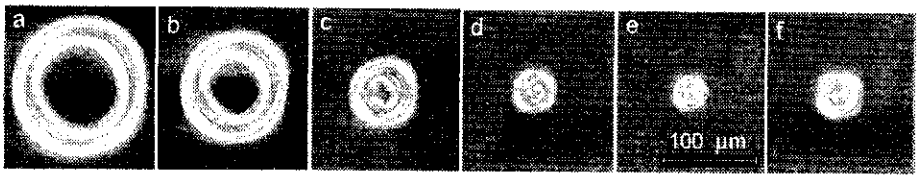

Fig. 8 Transformation of the CF-1 loop (a,b,c,d) into a cholesteric bubble (e,f). Mixture ROCHE 3421 + 0.64 % wt. S811; 50 °C, C = 1.9, d = 30 µm, f = 60 Hz; a,b) V = 5.705 V; c) V = 5.805 V; d) V = 6.503; e) $V = V_{tr}$ = 6.604 V; f) V = 5.604

pical phase diagram in a.c. electric field is given e.g. in Ref. [24].

Looped fingers (i.e. fingers forming closed loops) are sometimes observed in electro-optic cells. They grow while keeping a circular shape at voltages close below V_2 and start to undulate if the voltage is further decreased. At voltages higher than V_2 the radius of the loop slowly decreases. The loop transforms into a cholesteric bubble (spherulite) if the applied voltage is higher than V_{tr} (higher than V_2), being itself strongly dependent on the confinement ratio C. This transformation is discontinuous and irreversible, and operates only in thick cells (typically for $C > C_s \approx 1.2$) (Fig. 8). In thin cells ($C < C_s$) the loops collapse without forming bubbles [25,26].

CF-2 Fragments, Loops and Spirals

The CF-1's have been known for a long time because there are the easiest to obtain experimentally, especially in cells with small C (< 2). More recently, another type of fingers has been discovered, first in polymeric mixtures [27–30] and then in ordinary liquid crystals [9]. They are called cholesteric fingers of the second type or CF-2. They form spontaneously from the nematic phase in a thick sample ($C > 3$) after the voltage is abruptly decreased. These fingers differ from the CF-1's in many respects. For instance, a CF-2 segment has a point defect at each end [25] (Fig. 9) and does not systematically collapse in high electric fields or at small thickness as would do a CF-1, but rather forms a cholesteric bubble whose diameter is voltage dependent (Fig. 8 e,f) [26,31]. Conversely, a CF-2 segment can be obtained by "stretching" a cholesteric bubble by decreasing the voltage below a certain voltage V_s, which is lower than the coexistence voltage V_2 (typically 0.1 V below V_2) [32]. In that way, two pieces of a CF-1 with a rounded end start to grow from the bubble, which then splits to give a CF-2 segment embedded in a CF-1 finger (Fig. 10). An important point is that the CF-2 is energetically more favourable than the CF-1 at all voltages and systematically lengthens inside the

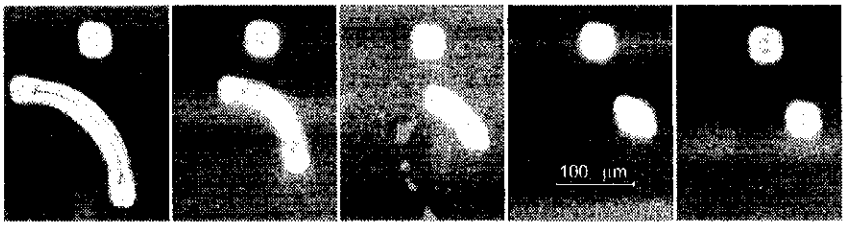

Fig. 9 Transformation of a CF-2 segment into a cholesteric bubble at voltage V = 5.605 V: Mixture ROCHE 3421 + 0.64 % wt. S811, 50 °C, f = 2 kHz, C = 1.93, p = 15.55 µm, V_2^* = 5.301 V. Duration of the transformation: about 5 minutes. Crossed polarizers

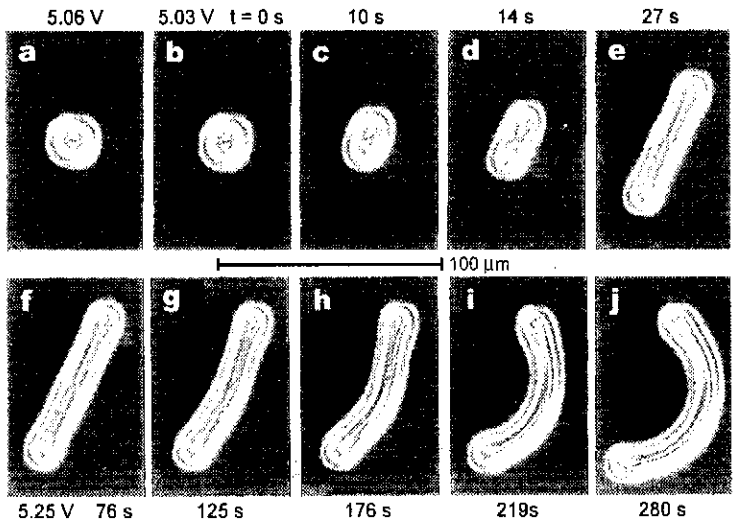

Fig. 10 Nucleation and growth of a CF-2 segment from a cholesteric bubble. The same mixture as in Fig. 8. V_2 = 5.25 V; crossed polarizers. (From Ref. [23])

CF-1. The velocity of the end of a CF-2 segment embedded in a CF-1 fragment, as well as the velocity of the CF-1 rounded tips are given as a function of the applied voltage in Fig. 11 [23].

The CF-2's can also drift perpendicularly to their axes in an a.c. electric field at voltage V_2^* which depends very slightly on the length of the fragment [23]. We emphasize that fragments, although observable during very long time, are unstable with respect to a length variation (and so are transient solutions): indeed too short fragments shorten, whereas too long ones lengthen. In addition their drift velocity depends on their length and shape (Fig. 12) [23].

More important is that the drift velocity of a CF-2 strongly depends on the

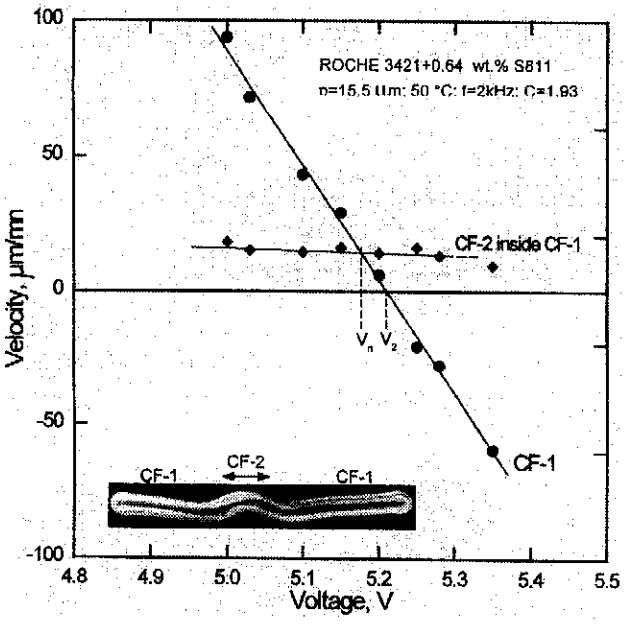

Fig. 11 Lengthening velocity of the CF-2 inside the CF-1 and lengthening velocity of the CF-1 as a function of the applied voltage. (From Ref. [23])

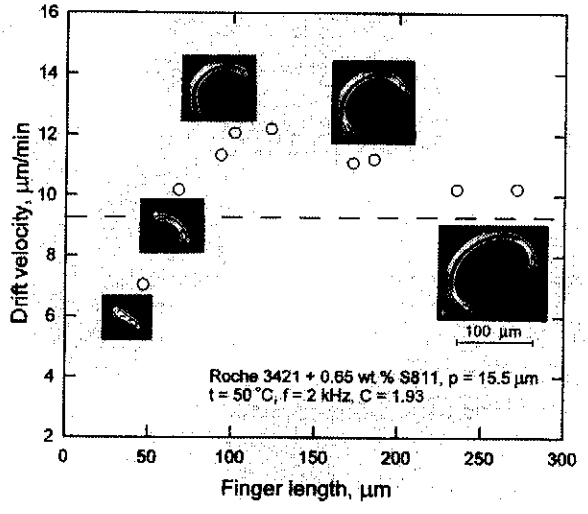

Fig. 12 Drift velocity as a function of the length of the CF-2 fragment. The dotted line gives the asymptotic drift velocity of a CF-2 in a well-developed spiral far from its centre. Crossed polarizers. (From Ref. [23])

electric conductivity of the liquid crystal chosen (Fig. 13). In particular, it vanishes exponentially when the frequency of the applied voltage is larger than the charge relaxation frequency of the sample [34]. In addition, it is proportional to the applied electric field (provided that the confinement ratio remains constant).

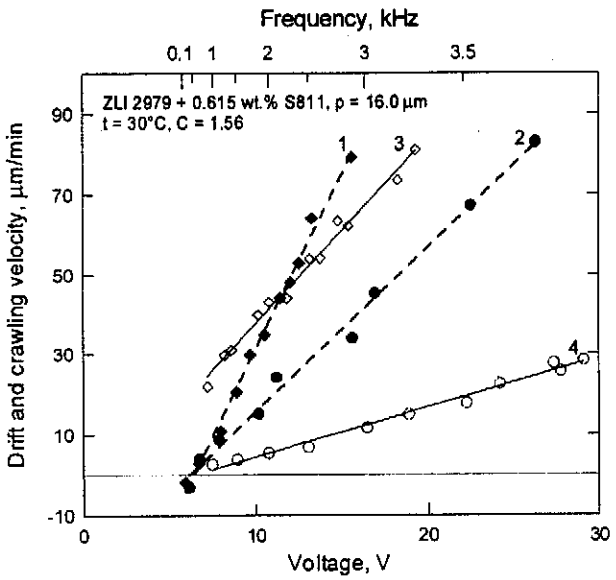

Fig. 13 Crawling velocity of a CF-1 *vs* voltage V_2 (1,2) and drift velocity of a CF-2 *vs* voltage V_2^* (3,4) in chiral mixtures of different electric conductivities. (1,3) $\sigma = 5.3\times10^{-9}$ Ω^{-1} cm^{-1}, (2,4) $\sigma = 2.8\times10^{-10}$ Ω^{-1} cm^{-1}. (Dependence of the dielectric anisotropy on frequency was used to change the coexistence voltage)

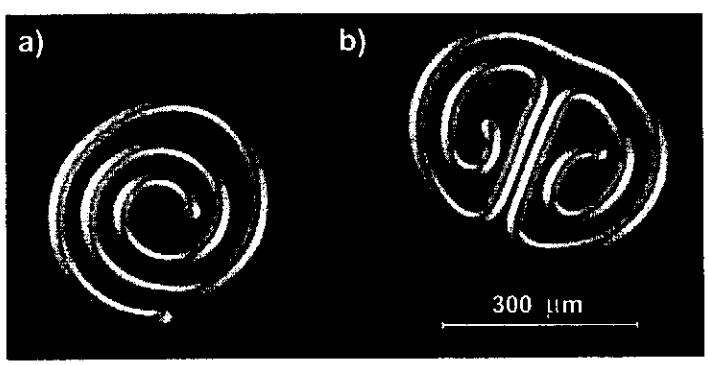

Fig. 14 Simultaneously growing single (a) and twin (b) spirals in the chiral mixture ZLI 2979 + 0,615 wt. % S811 (after 8 minutes): t = 30 °C, p = 16.0 µm, C = 1.84, V = 7.35 V, f = 100 Hz

At $V < V_2$ the fingers lengthen while drifting and form, depending on the initial condition, either single Archimedian spirals or twin spirals (Fig. 14). Twin spirals form preferentially close to V_2 and single ones close to some voltage $V_n < V_2$ [32]. Below V_n, CF-1 segments grow from both free ends of the spiral. If one end of the finger is attached (e.g. to a dust particle) and if the finger is initially long enough, a spiral can form at long time, even at voltages above V_2 [9].

For spirals with two free ends, their inner tips describe circles of finite radii with a constant velocity, while their outer tips describe logarithmic spirals (Fig. 15). By contrast, we observed that trajectories of the two tips are open above V_2 and resemble straight lines at V_2 (at this voltage, the tangential tip velocity $v_t \approx 0$). Above V_2 the total length of the spiral increases due to its drift in spite of the fact that the finger generally shortens from its two ends. Spiral dynamics is described in detail in Refs [25,35].

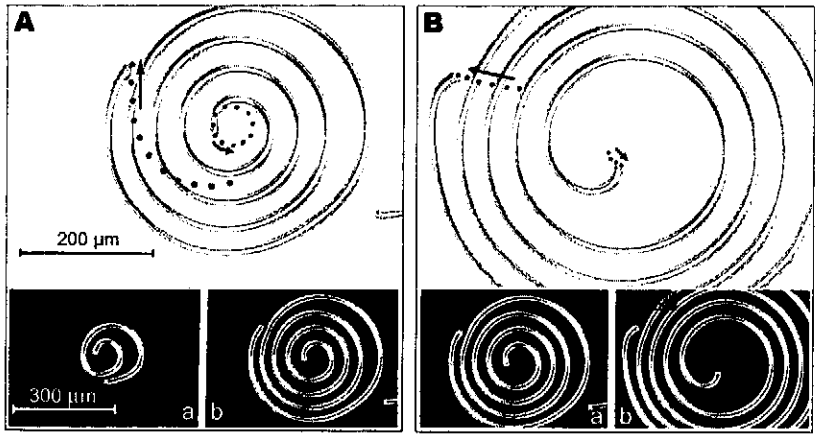

Fig. 15 Single spiral growing in the chiralized mixture Roche 3421 at $C = 1.93$; $d = 30$ µm, $t = 50$ °C, $f = 2$ kHz and different voltages ($V_2^* = 5.264$ V, $V = 5.25$ V): A) $V_2 = 5.144$ V, the inner tip describes a circle (at angular velocity 73° min^{-1}) and the outer tip a logarithmic spiral: a) $t = 0$ min; b) $t = 10$ min; B) $V = 5.240$ V, both tips describe an open trajectory: a) $t = 0$ min, $b = 9$ min; Dots on the shadow sketches show the tip trajectories.

A peculiar solution is observed just below V_2^*. In this case, short arched (staple-shaped) segments systematically develop as shown in Fig. 16. In that case, the central part of the finger continuously lengthens and flattens, while its two hooked ends remain similar and move away from each other [23].

In thick samples ($C > 2$–3) looped CF-2 fingers form sometimes spontaneously from the homeotropic nematic phase after switching the voltage below the spinodal limit V_0 of the nematic phase [23,25]. Each circular loop has

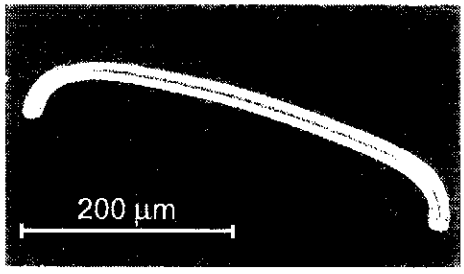

Fig. 16 Taple-shaped CF-2 finger in chiralized mixture ROCHE 3421 at 50 °C: C = 1.93, d = 30 µm, V = 5.263 V, f = 2 kHz, crossed polarizers

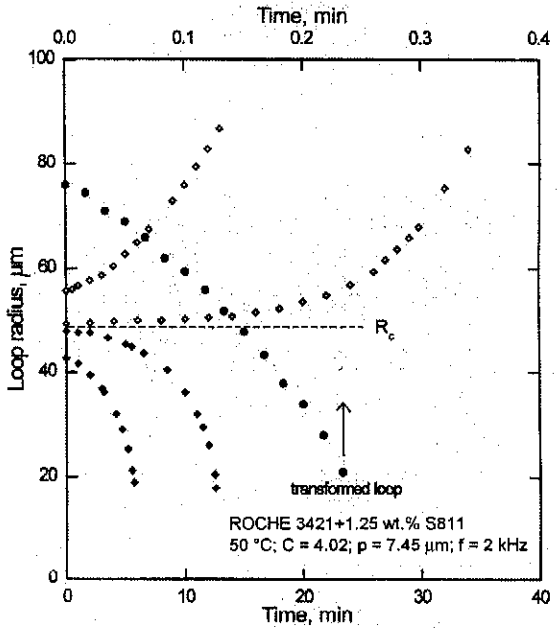

Fig. 17 Radius of a loop of a CF-2 as a function of time for different initial radii at V = 14 V. (From Ref. [23]).The non transformed loop grows or collapses depending on its initial radius (critical radius R_c is close to 47.5 µm). For comparison, the time evolution of a transformed loop at V = 14.65 V is plotted in the graph (note that the corresponding upper time scale is very different from the lower one)

a critical radius $R_c(V)$ above which it grows and below which it collapses (Fig.17).

The critical radius is proportional to the voltage and vanishes at V_2. A CF-2 loop never leads to a cholesteric bubble except when it contains a point defect.

In addition, it was shown experimentally and numerically that the CF-2's get abruptly thinner when the electric field exceeds the spinodal limit V_3 of the CF-1's

(Fig. 18). It has been observed that the collapse of a CF-2 loop is much faster after its thinning transition than before it (see Fig. 17). Note that this transformation is reversible, but strongly hysteretic [23,25,35].

Finally, it has been observed that below V_2, usual (i.e. non-transformed) CF-2 loops of large enough diameters spontaneously undulate (Fig. 19).

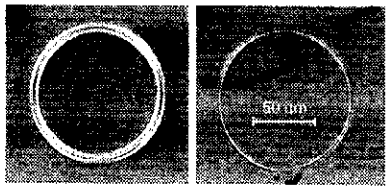

Fig. 18 Transformation (from left to right) of a CF-2 loop when a voltage $V > V_{tr}^{*}$ is applied: Roche mixture, t = 50°C, p = 7.45 µm, C = 4.02, f = 2 kHz, V_{tr}^{*} = 14.62 V. (From Ref. [23])

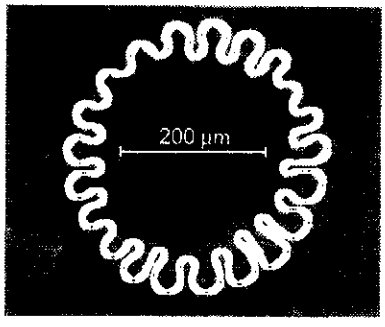

Fig. 19 Undulating CF-2 loop at voltage 11.4 V: Roche mixture, t = 50°C, p = 7.45 µm, C = 4.02, f = 2 kHz. The destabilization starts below voltage V_u = 11.65 V. Crossed polarizers

CF-3 and CF-4 Fragments

The properties of these fingers have not been investigated systematically up to now. The CF-3's are the thinnest ones while the CF-4's are the thickest ones. These fingers possess two disclination lines along their axes and do not move in an electric field contrary to CF-1's and CF-2's [10]. The director field inside a CF-3 possesses two twist disclination lines near the electrodes as shown in Fig. 4. Note that this molecular configuration was first proposed by Kléman and Cladis [36].

It has been observed that the sides of the CF-3's destabilize by undulating when the voltage is decreased below V_2. This instability is followed by the growth in the direction perpendicular to the finger axis of small elements of CF-1's: the CF-3 then resembles a zip (Fig. 20). CF-3's can also nucleate by forming spirals or loops when the sample is cooled down from its isotropic liquid in an a.c. electric field (Fig. 21).

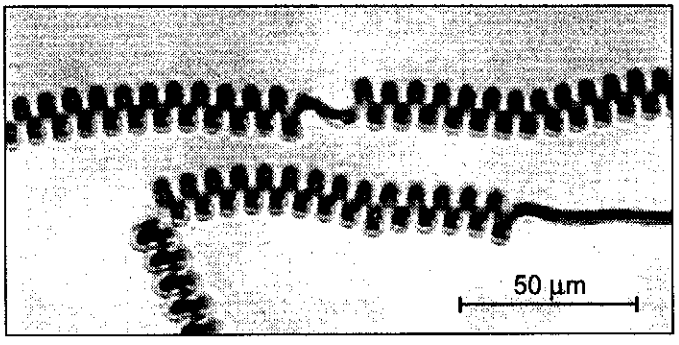

Fig. 20 Strong undulation of the CF-3 at voltage 6.968 V, slightly below V_2: 5CB + 3.21 wt. % CB15, t = 30 °C, p = 4.5 µm, f = 6 kHz, C = 4.44, parallel polarizers

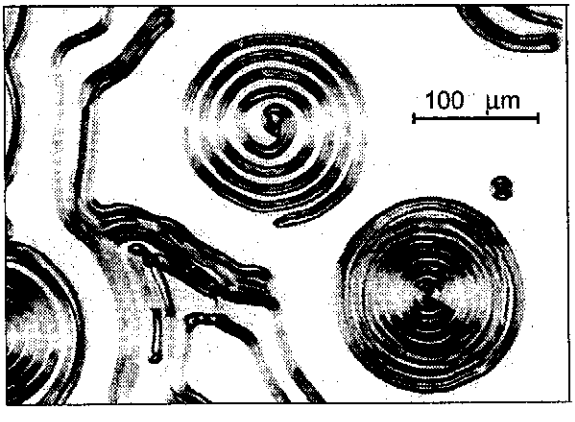

Fig. 21 Spirals and loops of CF3 obtained from the isotropic liquid by cooling down the electro-optic cell under voltage 1.9 V: Parallel polarizers, 5CB + 0.83 wt. % CB15, t = 30 °C, p = 17.95 µm, f = 100 Hz, C = 1.67

These spirals (contrary to the CF-2 spirals) are motionless, as their tips cannot move. In particular, it seems impossible to create and stabilize CF-3's with both free tips. In addition, their behaviour is rather complex. Indeed, they are sta-

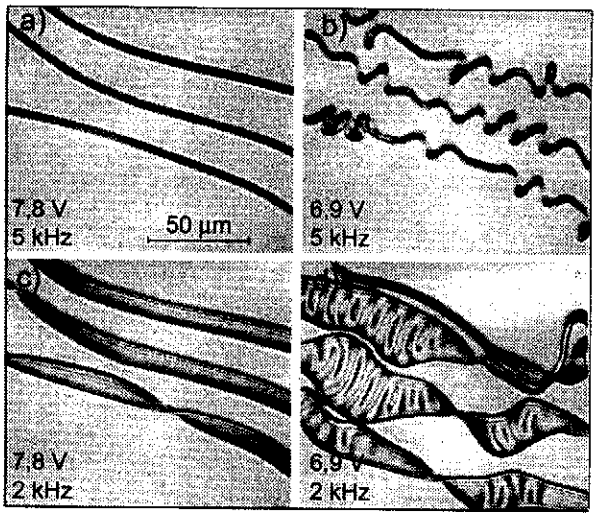

Fig. 22 Transformations of CF-3 fingers observed at different voltages and frequencies: 5CB + 3.21 wt. % CB15, t = 30 °C, p = 4.5 µm, C = 4.44, parallel polarizers

ble only if the voltage and the frequency exceed some threshold values (Fig. 22a). On the other hand, they destabilize at high frequency by undulating (Fig. 22b) when the voltage is decreased below some critical value close to V_2. If at high voltage, the frequency is decreased, the CF-3's start to form a ribbon. This instability is due to the distancing of the two disclination lines contained in the CF-3 (see Fig. 4) and to the formation of a planar region (inversion wall) in between (Fig. 22c); this wall can itself undulate if the voltage (or the frequency) are further decreased (Fig. 22d). All these transformations are reversible.

The CF-4's have been observed so far only during the directional solidification of the cholesteric phase from its isotropic liquid [10]. They occur to be stable only if their two tips are pinned. It has been observed many times that a CF-4 can partially detach from the front with the isotropic liquid: it then irreversibly transforms into a CF-3. A model for the director field of a CF-4 is shown in Fig. 4. As for the CF-3, it contains two twist disclination lines. The main difference between them is that the lines are close to the same electrode in the CF-4 whereas they are superimposed and located close to each electrode in the CF-3 (Fig. 4).

Conclusion

To conclude this article, we would like to mention that several mechanisms have been proposed for explaining the motion of the fingers of the first and of the second type in a low-frequency electric field. Among the mechanisms that have been proposed are the flexoelectric effect and the Lehman effect [33]. These two mechanisms cannot explain our observations as shown in [34]. On the other hand, Tarasov *et al.* developed recently an electrohydrodynamic model in very good agreement with our observations [37,38], confirming our expectations about the origin of the drift.

Acknowledgements

This work was supported by the Ministry of Education, Youth and Sports of Czech Republic under the research project VZ 253100001.

References

[1] Friedel G.: Annales de Physique **18**, 273 (1922).
[2] Bouligand Y.: J. Physique France **33**, 715 (1972).
[3] Brehm M., Finkelmann H., Stegemeyer H.: Ber. Bunsenges. Phys. Chem.**78**, 883 (1974).
[4] Kawachi M., Kogure O., Kato T.: Jap. J. Appl. Phys. **13**, 1457 (1974).
[5] Haas W.E.L., Adams J.E.: Appl. Phys. Lett. **25**, 263 and 535 (1974).
[6] Press M.J. , Arrott A.S.: J. Physique France **37**, 387 (1976).
[7] Press M.J. , Arrott A.S.: Mol. Cryst. Liq. Cryst. **37**, 81 (1976).
[8] Hirata S., Akane T., Tako T.: Mol. Cryst. Liq. Cryst. **38**, 47 (1981).
[9] Ribière P., Oswald P., Pirkl S.: J. Phys. II (France) **4**, 127 (1994).
[10] Baudry J., Pirkl S., Oswald P.: Phys. Rev. E **57**, 3038 (1998).
[11] Pirkl S.: Cryst. Res. Technol. **26** (3), 371 (1991).
[12] Pirkl S.: Cryst. Res. Technol. **26** (5), K 111 (1991).
[13] Blinov L.M.: *Electro-optical and Magneto-optical Properties of Liquid Crystals,* Wiley, New York, 1983.
[14] De Gennes P.G., Prost J.: *The Physics of Liquid Crystals,* Clarendon, Oxford, 1993.
[15] Oswald P., Pieranski P.: *Les Cristaux Liquides, Tome 1: Concepts et propriétés physiques illustrés par des expériences*, Gordon and Breach Sci.Pub., Paris, 2000. (English version in press at Taylor & Francis).
[16] Ribière P., Pirkl S., Oswald P.: Phys. Rev. A **44** , 8198-8209 (1991).

[17] Pirkl S., Tuček J., Ribičre P., Oswald P.: Proc. Eurodisplay '93, 297-300 (1993)
[18] Pirkl S.: Cryst. Res. Technol.: **28** (7), 1027-38 (1993)
[19] Lequeux F., Oswald P., Bechhoefer J.: Phys. Rev. A **40**, 3974 (1989).
[20] Ribière P., Oswald P.: J. Physique France **51**, 1703 (1990).
[21] Ribière P., Pirkl S., Oswald P.: Liq. Cryst. **16**, 203 (1994).
[22] Stieb A.: J. Physique France **41**, 961 (1980).
[23] Pirkl S., Oswald P.:Liq. Cryst. **28**, 299 (2001).
[24] Pirkl S.: Liq. Cryst. **16**, 973 (1994).
[25] Baudry J., Pirkl S., Oswald P.: Phys.Rev. E **59**, 5562 (1999).
[26] Pirkl S., Ribiere P., Oswald P.: Liq.Cryst. **13**, 413 (1993)
[27] Gilli J.M., Kamayé M.: Liq. Cryst. **11**, 791 (1992).
[28] Gilli J.M., Kamayé M.: Liq. Cryst. **12**, 545 (1992).
[29] Mitov P., Sixou P.: J. Phys. II France **2**, 791 (1992).
[30] Mitov P., Sixou P.: Mol. Cryst. Liq. Cryst. **231**, 11 (1993).
[31] Kawachi M., Kogure O., Kato Y.: Jap. J. Applied. Phys. **13**, 1457 (1974).
[32] Pirkl S., Oswald P.: J. Phys. II (France) **6**, 355 (1996).
[33] Gil L., Gilli J. M.: Phys. Rev. Lett. **80**, 5742 (1998).
[34] Baudry J., Pirkl S., Oswald P.: Phys.Rev. E **60**, 2990 (1999).
[35] Oswald P., Baudry J., Pirkl S.: Physics Reports **337**, 67 (2000).
[36] Cladis P.E., Kléman M.: Mol.Cryst.Liq.Cryst. **16**, 1 (1972).
[37] Tarasov O.S.: *Stuctural Transitions and Dynamics of Liquid Crystals under Flows and Electric Fields*, PhD Thesis, University of Bayreuth, 2003.
[38] Tarasov O.S., Krekhov A.P., Kramer L.: Phys. Rev. E **68** (3), 031708 (2003).